Title

THE MULTI-VIEW FOG PROGRAM AND ITS APPLICATION TO QUALITY CONTROL OF FSD DATA

Authors

Buckman, Shirley
Franz, Joan
Gotthelfsman, John
et al.

Publication Date

1965-10-01

UCRL-16508

University of California

Ernest O. Lawrence Radiation Laboratory

THE MULTI-VIEW FOG PROGRAM
AND ITS APPLICATION TO QUALITY CONTROL OF FSD DATA

DISCLAIMER

Conf. on Programming for Flying
Spot Devices, Columbia University

UCRL-16508

Also UCID 2652

UNIVERSITY OF CALIFORNIA
Lawrence Radiation Laboratory
Berkeley, California

AEC Contract No. W-7405-eng-48

THE MULTI-VIEW FOG PROGRAM AND ITS APPLICATION TO QUALITY CONTROL OF FSD DATA

Shirley Buckman, Joan Franz, John Gotthelfsman,
Dennis Hall, Vivian Morgan and Frank Windorski

October 1965

The Multi-View FOG Program and its Application to Quality Control of FSD Data

Shirley Buckman, Joan Franz, John Gotthelfsman, Dennis Hall, Vivian Morgan and Frank Windorski

I. Introduction

One of the most difficult problems encountered in the reduction of Bubble Chamber data is that of quality control. In particular, the problem of detecting FILTER errors is especially difficult. This is due in part to the fact that FILTER errors, by definition, do not depart from the true orbit by more than a road width (at Berkeley, 512 μ) and are usually smaller than half a road width. Hence, this kind of error is by nature more subtle than analogous errors made by a Frankenstein operator or a faulty digitizer.

For this reason, if we are to have any hope of detecting these errors, it is necessary to have an accurate model of the true orbit on the film. If the number of erroneous points is sufficiently small in relation to the total number of points measured, then a maximum likelihood fit to such a model will show erroneous points as significantly displaced from their expected values.

The term "significantly displaced" means that the displacement is much larger than would be expected on the basis of an a priori error estimate. Hence, a second requirement for the detection of FILTER errors is that there exist predictable confidence intervals for all error sources.

More precisely, the following information is required:

A. An accurate relationship which gives the FSD film coordinates ξ' of a point X on the orbit as a function of the initial conditions for the particle and, say, the arc length s of X as measured along the orbit from the initial position of the particle.

B. Predictable confidence intervals for all acceptable error sources.

Multi-view FOG, an extension of the current 2-view FOG program, will provide a maximum likelihood estimate of the momentum and position vectors of a track near a vertex. It will also provide a reliable discrimination function which will separate good measurements from bad measurements on a statistical basis and will under certain conditions attempt to remove bad points from a track.

II. Mathematical Model

Consider a particle in a bubble chamber with initial position vector X_v and initial momentum vector $P_v = p_v\lambda_v$, where p_v is the momentum scaler and λ_v the unit tangent vector at the vertex. The forces which significantly affect the position of the particle are the following:

The magnetic field force, $(qB) \times (v\lambda)$, where B is the instantaneous magnetic field vector, v is the instantaneous velocity scaler, λ is the instantaneous tangent vector, and q is the charge on the particle. (1)

Ionization energy loss, $\frac{dp}{dt}\lambda$, where p is the instantaneous momentum scaler. (2)

Elastic collisions with other particles. Because of the random nature of this force, it will be treated as one source of error. (3)

From the forces 1 and 2 on the particle it is possible to derive a functional relationship between the instantaneous position vector X and the variables s, P_v and X_v. (s = arc length from X to X_v).

In Appendix A, an approximation $\overline{X}(s)$ to the true orbit X(s) is derived.

$$\overline{X}(s) = \overline{X}_i(u) = X_i + \lambda_i u + V_i\,\overline{S}(u) + W_i\,\overline{C}(u) \qquad (4)$$

where

$$ih \leq s \leq (i+1)\,h$$
$$u = s - ih$$
$$X_i = \overline{X}_{i-1}(h), \quad X_o = X_v$$
$$\lambda_i = \overline{\lambda}_{i-1}(h), \quad \lambda_o = \lambda_v$$
$$V_i = (B_i \times \lambda_i)/\,|B_i|$$
$$W_i = (B_i \times V_i)\,/\,|B_i|$$

and $\overline{S}(u)$, $\overline{C}(u)$ are scaler functions of u.

Clearly, (4) is not particularly difficult to evaluate. The only differences between (4) and a circular helix are the functions $\bar{S}(u)$ and $\bar{C}(u)$. For circular helices, these functions are simple sines and cosines. For the approximation (4) they involve natural logarithms as well. Preliminary indications are that the evaluation of (4) together with all of its partial derevatives will require about one millisecond per point on the IBM 7094-II.

It is also shown in Appendix A that for every ϵ there exists an h such that

$$|X(s) - \bar{X}(s)| \leq \epsilon \text{ whenever } ih \leq s \leq (i+1)h \tag{5}$$

In fact it is shown that (5) will be satisfied whenever

$$h \leq \left[\frac{\epsilon}{\frac{C\ L\ q\ |B_v|}{10\ p_v}}\right]^{1/3} \tag{6}$$

where L is the total length of measured track and

$$C = \frac{|B_v''|}{|B_v|} - \left(\frac{|B_v'|}{|B_v|}\right)^2 + \frac{p_v''}{p_v} - \left(\frac{p_v''}{p_v}\right)^2 \tag{7}$$

Thus, given an ϵ, we can compute an h such that condition (5) is satisfied. By choosing ϵ sufficiently small the correct model of the space orbit is obtained.

The two dimensional analogue of (4) without condition (5) is derived by Solmitz[1] for the program TVGP.

Table I gives h and $N = \frac{L}{h}$ as a function of p_v and L for some typical cases using $\epsilon = 30\mu$ in space, the mass of a π, and the magnetic field of the 72" Hydrogen Chamber.

The chief advantage of this model is that it is self regulatory. That is, even with large changes of field and long stopping tracks, constant accuracy will be maintained. Hence, this source of error is eliminated.

As a consequence of this the program running time is improved, since most tracks will only require between 1 and 3 splice points.

Now consider the relationship between a point X in space and its image ξ on film. The approach taken in multi-view FOG is to assume an approximate model, and from this determine confidence intervals from fiducial measurements. Appendix B gives a derivation for a simple optical model of the form:

TABLE OF INTERVAL SIZES FOR ORBIT MODEL

p \ L	10 cm		30 cm		90 cm	
3.0 BeV/c	$h \leq 23.5$	$N = 1$	$h \leq 18.0$	$N = 2$	$h \leq 14.4$	$N = 7$
0.5 BeV/c	$h \leq 15.6$	$N = 1$	$h \leq 12.82$	$N = 3$	$h \leq 10.0$	$N = 9$
0.1 BeV/c	$h \leq 2.16$	$N = 5$	$h \leq 1.5$	$N = 20$	not possible	

h = maximum interval size

N = number of intervals

L = total length of measured track

p = initial momentum

ϵ = 30 microns in space

$|B_v|$ = 17.5 kilogauss

mass = .135 BeV

$$h = \left[\frac{\epsilon}{c \frac{L}{10} \frac{g|B_v|}{pv}} \right]^{1/3}$$

$$c \leq \frac{|B_v|''}{|B_v|} - \left(\frac{|B_v|'}{|B_v|} \right)^2 + \frac{p_v''}{p_v} - \left(\frac{p_v'}{p_v} \right)^2$$

$$F_L(X,\xi) = 0 \tag{8}$$

This model is adequate for all chambers currently being processed at Berkeley. However, it is anticipated that some future chambers may be quite different in structure. Therefore, the program has been designed so that this module can be replaced easily.

Equations (4) and (8) give, as a function of arc length s in space, a relationship between the initial conditions of a particle and the coordinates ξ of its image on the film. To complete requirement A it is necessary to obtain the relationship between film coordinates ξ and FSD coordinates ξ'.

It is assumed that

$$\begin{pmatrix} \xi \\ \eta \end{pmatrix} = \begin{pmatrix} a & b \\ c & d \end{pmatrix} \begin{pmatrix} \xi' \\ \eta' \end{pmatrix} + \begin{pmatrix} e \\ f \end{pmatrix} \tag{9}$$

That is, film coordinates differ from FSD coordinates by a translation, a rotation, a shear and an independent magnification in both ξ' and η'. The coefficients a, b, c, d, e and f are determined independently for each photograph by a least squares fit to the measured fiducials. From (4), (8), and (9) we have all of the information required for A.

III. Error Analysis

The next problem is that of determining confidence intervals. The errors caused by the magnetic field and range-momentum models are insignificant for all chambers currently being processed at Berkeley. However, the procedure could easily be extended to include them should they be significant in some new chamber. Chamber turbulance is a slight problem, but we shall ignore it for the present.

The following list enumerates all error sources presently being considered.

a. Multiple scattering.
b. Incorrect optical model.
c. Film resolution and FSD accuracy.
d. Incorrect fiducial measurement.
e. Undetected FILTER errors or bit transmission error.
f. Wrong mass hypothesis.

(10)

Data containing errors from sources (a) through (c) are acceptable. Data containing errors from sources (d) through (f)

are unacceptable. Hence, it is therefore necessary to have a reliable method for detecting their presence.

The first problem is that of multiple scattering. Rossi[2] gives the following approximation to the average error (d) due to neglecting (3).

$$d \sim \frac{.24}{p\beta} \left(\frac{S}{X_o}\right)^{3/2} \tag{11}$$

where

X_o = radiation length in cm.

$\beta = p/E$

E = energy = $\sqrt{p^2 + (\text{mass})^2}$

The projection of d onto the xy plane will be $\frac{2}{\pi}$ d on the average and hence on the film the average deviation d_{fm} is given by

$$d_{fm} = \frac{2}{\pi} d \Big/ G(p,Z) = .15 \left(\frac{S}{X_o}\right)^{3/2} \Big/ p\beta \cdot G(p,Z) \tag{12}$$

The second error source is the optical model. This problem is quite chamber dependent, and it is hard to give a general procedure for determining the error. The procedure to be employed for all chambers currently being processed is the following:

To determine the coefficients of the optical model, all of the fiducials in a picture will be measured several times and a least squares fit to the optical coefficients will be performed. This procedure yields residuals for each fiducial. If these residuals are randomly distributed about zero at each fiducial, and if they have a magnitude comparable to the rms error of the measuring device, the optical model is "exact" and this source of error can be eliminated. If, on the other hand, the residuals are not randomly distributed about zero, there is an error in the optical model. This source of error must be accounted for either by improving the model, or by giving up and admitting that the error on a point on the film is actually greater than the maximum accuracy of the measuring machine. If the latter approach is taken, a good estimate for this error source is obtained by computing the average deviation e_{f_i} for each fiducial i. Since the residuals were obtained as least squares fits,

$$\sum_{i=1}^{m} \bar{e}_{f_i} \sim 0 \text{ where } \bar{e}_{f_i} = \left(e_{\xi_{f_i}} \quad e_{\eta_{f_i}}\right)^T \tag{13}$$

Hence

$$\sigma^2_{optics} \sim \frac{\sum \bar{e}^2_{f_i}}{n} = \left(\frac{\sum \bar{e}^2_{\xi f_i}}{n} \quad \frac{\sum \bar{e}^2_{\eta f_i}}{n} \right)^T \tag{14}$$

The third error source is the resolution of the film and the rms scatter of the FSD itself. For the present time this is assumed to be constant, although in the future it may be desirable to add a refinement which would allow for the variation due to the angle the track makes with the scan line. Now, each master point is the average of one or more individual digitizing. Hence we have:

$$\sigma^2_\xi = \frac{\sigma^2_{FSD}}{M_\xi} = \left(\frac{\sigma^2_{\xi_{FSD}}}{M_\xi} \quad \frac{\sigma^2_{\eta_{FSD}}}{M_\xi} \right)^T \tag{15}$$

where M_ξ = number of points averaged in the master point. This relation is quite important in performing least squares fits, since the more accurate points are given a smaller error, and hence a higher weight.

This completes the task of assigning confidence intervals to all acceptable error sources. We now turn to the problem of dealing with the remaining errors.

The fourth error source is that of incorrect fiducial measurements. The coefficients of 9 are determined by performing a least squares fit. Since an a priori estimate of the error in fiducial measurements is known (for the Berkeley FSD, $\sigma_{FID} = (1.5\mu, 1.5\mu)^T$) it is possible to compute a χ^2 value for the fit.

Following Mood[3] we can test whether or not the measurement is consistent with the known standard deviation. Most bad fiducial measurements can be detected in this manner. Furthermore, since an a priori density function for the amount of shear and stretch for any particular film base, is also known, bounds may be placed on these parameters as well. This procedure will virtually guarantee every fiducial measurement.

It is worth noting that this test is much more powerful if the effects of an erroneous optical model are removed. Thus, if ξ_{f_i} is the cordinate of the fiducial predicted by the optical model, then

the least squares fit should be performed on the variable $\xi_{f_i} + \bar{e}_{f_i}$.

All of the acceptable error sources can be included at the discresion of the experimentor in the weighting matrix for the maximum likelihood fit. Thus there will be terms for multiple scattering, the number of individual digitizings used in the master point, and the optical model.

The multiple scattering term is of particular significance in heavy liquids and in long chambers. The optics term and the number of digitizings term are useful in the detection of FILTER errors.

IV. Constraints

Conditions A and B have now been satisfied. Hence a maximum likelihood determination of the initial conditions can be performed. (See Appendix C). This procedure will give a χ^2 value for the fit, which can be used to discriminate between bad measurements and good measurements. This process will introduce two types of errors.

I. Rejection of good measurements

II. Acceptance of bad measurements

Let P_I equal the probability of type I error and P_{II} equal the probability of type II error. P_I can be determined by integrating the χ^2 distribution. Again following Mood[3], the discrimination function consists of rejecting all events with $P_I \geq A$ and accepting all events with $P_I \leq A$, where A is an arbitrary constant assigned by the experimentor.

The trouble with this test is that it is not possible to minimize both error types simultaneously. Furthermore, the more P_I is decreased the greater P_{II} becomes. Making P_I extremely small is therefore undesirable from the standpoint of accuracy. On the other hand, the smaller P_{II} becomes, the larger P_I becomes. Hence the number of unnecessary remeasurements increases. Making P_{II} extremely small is therefore undesirable from the standpoint of economics.

Consider a track which has $P_I \geq A$ for all mass hypotheses. Four possibilities exist.

a. The event is actually good.
b. There was an undetected fiducial error.
c. There was an undetected track measurement error.
d. The correct mass hypotheses was not attempted.

(16)

Our experience indicates that such occurrances are most probably due to 16c errors. For this reason the program will attempt to decide whether this condition is likely. If it is, the program will have the option of deleting the bad points and repeating the fit, provided this can be done without serious loss of accuracy and information. In this way, the frequency of type I errors can be substantially reduced.

In order to determine a good test for the existence of an undetected measurement error we must first describe its characteristics. This is a very difficult task, requiring the acquisition of considerable additional experience with the residual distributions. This point has been emphasized by Paul Hough[4] and others. For this reason, the program will display the residuals for each track as a function of view, if requested. It will also display on request the weighted residuals so that probability tests can be made.

There is one final error source which cannot be detected by considering the point distribution. That is the problem of finding a vertex point. If the point of arc length zero, is incorrect then the initial conditions determined will not represent the true state of the particle at the vertex.

The actual computation of a vertex point will be done in CLOUDY as follows: For each track j at a vertex we have an orbit function $\bar{X}^j(s)$. The point X in space which is closest to all of the functions will be taken as the true vertex point. The point X_j on each orbit which is closest to X will be taken as the vertex point for that track. See figure.

Let λ_j be the tangent vector of the orbit at the point X_j. Then the distance δ_j from a point X' to this line is given by:

$$\delta_j = (\lambda^j)^T (X' - X^j) \tag{17}$$

The point X' satisfies the condition

$$\Sigma_j \delta_j^2 = \text{minimum} \tag{18}$$

PROGRAM 140

MULTI-VIEW FOG

GENERAL FLOW CHART

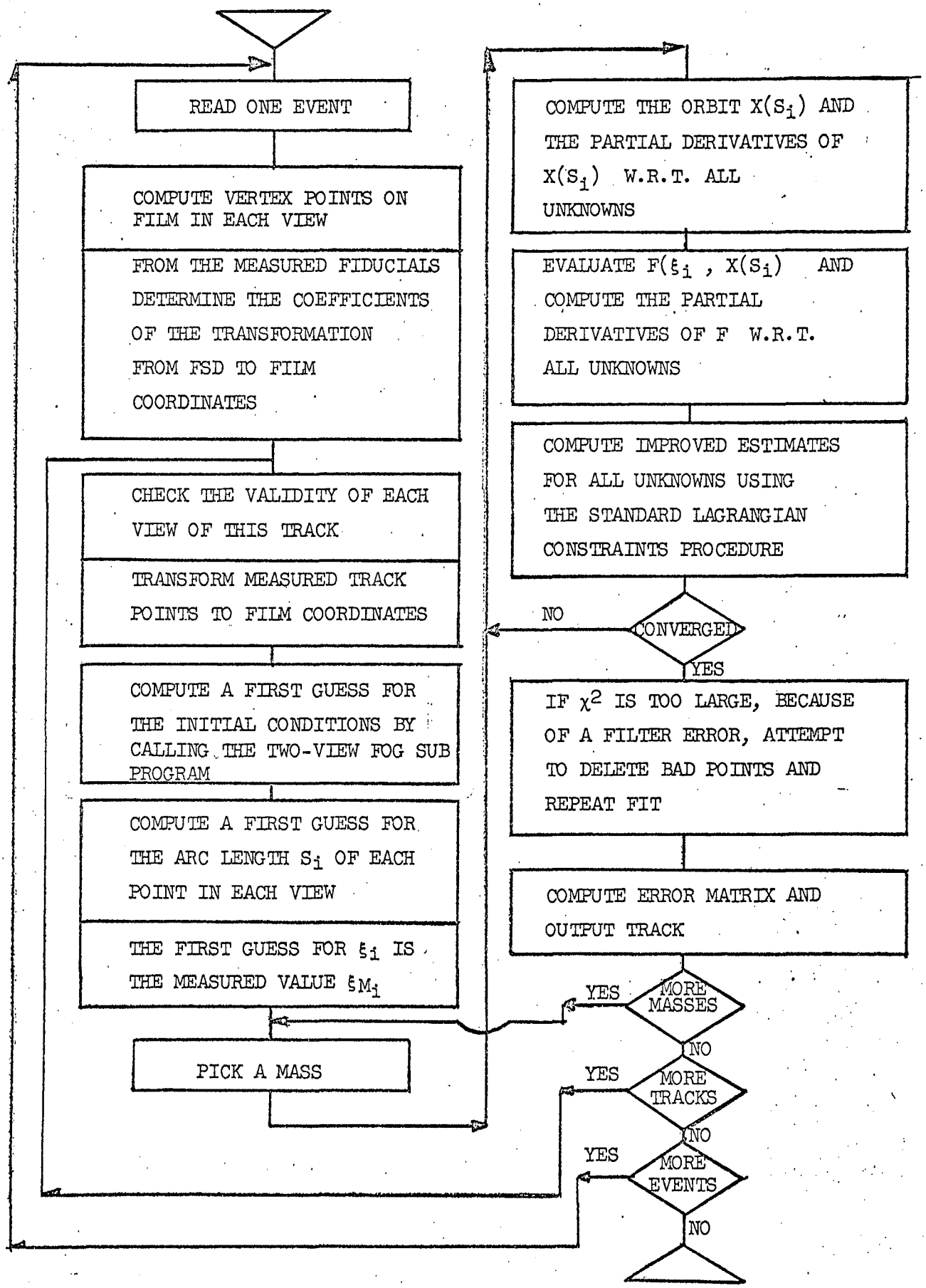

If it is assumed that X was actually determined from condition (18) and that the only source of error on X is due to errors on X_j, an error matrix for X is determined. (See Appendix D).

$$E_x = \sigma^2 \left[\sum_j \lambda_j \lambda_j^T \right]^{-1} \tag{19}$$

In particular, for the case of two tracks, the error is minimized when the tracks are orthogonal, and becomes infinite when the tracks are parallel. This result is of particular significance for neutral connecting tracks where an estimate of vertex points accuracy is needed in order to determine the errors on the direction of the line of flight.

Summary

The multi-view FOG program will produce maximum likelihood estimates for the momentum and position vectors at a vertex. These estimates will be as accurate as the resolution of the particular chamber being used. The program will also provide a discrimination function which will reliably separate good measurements from bad measurements. It will also attempt to detect and repair measurement errors so that the overall output of the FSD - HAZE system will be substantially improved.

Finally, multi-view FOG will be available for use with the Franckenstein system and the DAPR system as well, since all of the features are directly applicable.

Appendix A

Derivation of an approximation $\bar{X}(s)$ to the true orbit $X(s)$ of a particle in a bubble chamber.

Only magnetic field force, and momentum loss due to ionization will be considered.

From Newton's first law:

$$\frac{d(p\lambda)}{dt} = \frac{dp}{dt}\lambda + p\frac{d\lambda}{dt} = q(B \times v\lambda) + \frac{dp}{dt}\lambda \tag{1}$$

where $X = X_v$, $p = p_v$, $\lambda = \lambda_v$ at $t = 0$.

Thus

$$p\frac{d\lambda}{dt} = p\frac{d\lambda}{ds}\frac{ds}{dt} = p\frac{d\lambda}{ds}v = q(B \times v\lambda) \tag{2}$$

Hence

$$\frac{d\lambda}{ds} = q\frac{(B \times \lambda)}{p} \tag{3}$$

Define matrices M and Q as follows:

$$M = \begin{bmatrix} 0 & -B_z & B_y \\ B_z & 0 & -B_x \\ -B_y & B_x & 0 \end{bmatrix} ; \quad Q = \frac{qM}{p} \tag{4}$$

Then

$$\frac{d\lambda}{ds} = Q\lambda \tag{5}$$

Hence

$$\lambda = \lambda(s) = \mathrm{EXP}\left(\int_0^s Q dt\right)\lambda_v \tag{6}$$

But

$$\lambda = \frac{dX}{ds}$$

Hence

$$X = X(s) = X_v + \int_0^s \left[\text{EXP} \left(\int_0^v Q dt \right) \right] dv \tag{7}$$

The integration of λ is impossible to carry out except for very special forms of Q. Most geometry programs take the approach of assuming some simple integrable form $\overline{Q}$ for Q and calling the result the orbit. One such form is that suggested by Solmitz, Day and Johnson.[1]

$$\overline{Q} = \frac{Q_v}{1 - k_v t} \tag{8}$$

when t = arc length cm,

and $k \sim \left(\frac{q|B_v|}{p_v} \right)$

Then (6) becomes

$$\overline{\lambda}(s) = \text{EXP} \left[\frac{-Q_v}{k_v} \ln (1 - k_v s) \right] \lambda_v$$

$$\overline{\lambda}(s) = \lambda_v + \left(\frac{Q_v}{K_v} \right) \sin K_v \psi(s) + \left(\frac{Q_v}{K_v} \right)^2 (1 - \cos K_v \psi(s)) \tag{9}$$

where $K_v = \frac{q|B_v|}{p_v}$; $\psi(s) = \frac{-1}{k_v} \ln (1 - k_v s)$

And integrating (7)

$$\bar{X}(s) = X_v + \lambda_v s + \left(\frac{Q_v}{K_v}\right)\bar{S}(s) + \left(\frac{Q_v}{K_v}\right)^2 \bar{C}(s)$$

$$\bar{S}(s) = \int_0^s \sin K_v\psi(t)dt$$

$$= \left[k_v s + (1 - k_v s)(1 - \cos K_v\psi(s)) - \frac{k_v(1 - k_v s)}{K_v} \sin K_v\psi(s)\right] \div \Delta$$

$$\bar{C}(s) = \int_0^s (1 - \cos K_v\psi(t))dt \qquad (10)^*$$

$$= \left[- K_v s + \frac{k_v(1 - k_v s)}{K_v} (1 - \cos K_v\psi(s)) + (1 - k_v s) \sin k_v\psi(s)\right] \div \Delta$$

$$\Delta = K_v\left[1 + \left(\frac{k_v}{K_v}\right)^2\right]$$

---

* One could derive (10) by noting that

$$\bar{\lambda}(s) = (1 - k_v s)^{-\frac{Q_v}{k_v}} \lambda_v$$

Thus

$$\bar{X}(s) = X_v - \frac{1}{k_v}\left[I - \frac{Q_v}{k_v}\right]^{-1}\left[\left((1 - k_v s)^{-\frac{Q_v}{k_v}+I}\right)\lambda_v - \lambda_v\right]$$

$$= X_v + \left[Q_v - k_v I\right]^{-1}\left[(1 - k_v s)\bar{\lambda}(s) - \lambda_v\right]$$

The disadvantage to this equation is that as $k_v \to 0$, $\bar{X}(s)$ becomes indeterminate.

The multi-view FOG program uses spliced functions of the form A-8 over intervals short enough to guarantee that the maximum error over the entire track is less than a specified constant ϵ.

One can derive a good estimate for the error introduced in one splice interval as follows:

Let Θ represent the angle between the tangent vector and the projection of the X axis onto the osculating plane. Then

$$\frac{d\Theta}{ds} = \frac{1}{\rho} = \frac{q|B|}{p} \sim \frac{q|B_0|}{p_0}(1 + as + bs^2) \tag{11}$$

where $a = \dfrac{|B_0'|}{|B_0|} - \dfrac{p_0'}{p_0}$

$$b = \left(\frac{|B_0'|}{|B_0|} - \left(\frac{p_0'}{p_0}\right)\right)^2 + \left(\frac{|B_0''|}{|B_0|} - \left(\frac{|B_0'|}{|B_0|}\right)^2\right) + \left(\frac{p_0''}{p_0} - \left(\frac{p_0'}{p_0}\right)^2\right)$$

For the Solmitz approximation we have

$$\frac{d\Theta}{ds} = \frac{q|B_0|}{p_0(1 - k_0 s)} \sim \frac{q|B_0|}{p_0}(1 + k_0 s + k_0^2 s^2 + \ldots) \tag{12}$$

If we choose $k_0 = a$, then

$$\frac{d|\Theta - \bar{\Theta}|}{ds} \sim \frac{q|B_0|}{p_0} Cs^2 \tag{13}$$

where $C = b - k_0^2 = \dfrac{|B_0''|}{|B_0|} - \left(\dfrac{|B_0'|}{|B_0|}\right)^2 + \dfrac{p_0''}{p_0} - \left(\dfrac{p_0'}{p_0}\right)^2$

Clearly

$$d|X - \bar{X}| \sim \tan(\Theta - \bar{\Theta})\, ds \sim (\Theta - \bar{\Theta})\, ds$$

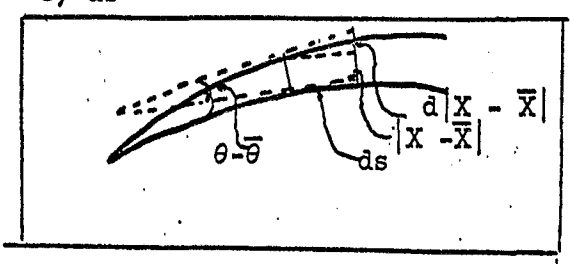

Hence

$$|X - \bar{X}| \sim \frac{q\,|B_0|\,C}{p_0}\,\frac{s^4}{3\times 4} \qquad (14)$$

Equation A-14 gives a good estimate of the departure of the true orbit from the Solmitz approximation in the osculating plane. The other component of error is normal to this plane.

An xyz coordinate system is chosen so that the xy plane coincides with the osculating plane at s = 0.

Let

φ be the dip angle in this system

Θ be the azimuth angle in this system.

From the differential equation A-5 we have:

$$\frac{d^2z}{ds^2} = \frac{q}{p}\left[B_x \frac{dy}{ds} - B_y \frac{dx}{ds}\right]$$

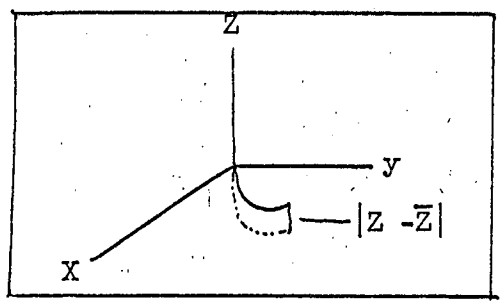

Now

$$B_x = |B| \sin \varphi_B \cos \Theta_B$$

$$B_y = - |B| \sin \varphi_B \sin \Theta_B$$

$$\frac{dx}{ds} = \cos \Theta$$

$$\frac{dy}{ds} = - \sin \Theta$$

Therefore

$$\frac{d^2z}{ds^2} = \frac{q|B|}{p}\left[- \sin \varphi_B \cos \Theta_B \sin \Theta + \sin \varphi_B \sin \varphi_B \cos \Theta\right]$$

$$\frac{d^2z}{ds^2} = - \frac{q|B|}{p} \sin \varphi_B \sin (\Theta - \Theta_B)$$

The total error E for a segment of length h is given by

$$E = |X - \bar{X}| + |Z - \bar{Z}| = \frac{q|B_0|C}{p_0}\left[1 + \frac{q|B_0|}{p_0}\sin\varphi_{B_0}\,\frac{h}{5}\,\frac{h^4}{3.4}\right]$$

$$\leq .1\,\frac{q|B_0|}{p_0}\,Ch^4$$

for most tracks.

The error introduced in N such segments is

$$NE = \frac{.1Nq|B_0|\,Ch^4}{p_0} < \epsilon$$

If the track has length L in space and we want $h = \frac{L}{N}$ or $N = \frac{L}{h}$

Then $$\frac{.1qL|B_0|\,Ch^3}{p_0} < \epsilon$$

Hence $$h < \left[\frac{\epsilon}{\frac{.1qL|B_0|\,C}{p_0}}\right]^{1/3}$$

Appendix B

Derivation of a Simple Optical Model for the Projection of Space to Film

The following assumptions are made:

1. All material interfaces are perpendicular to the lens axis.
2. There are $n + 1$ such interfaces.
3. The Z axis is chosen parallel to the optic axis.
4. The lens properties can be approximated by a pinhole on the back of a refractive material of constant thickness.

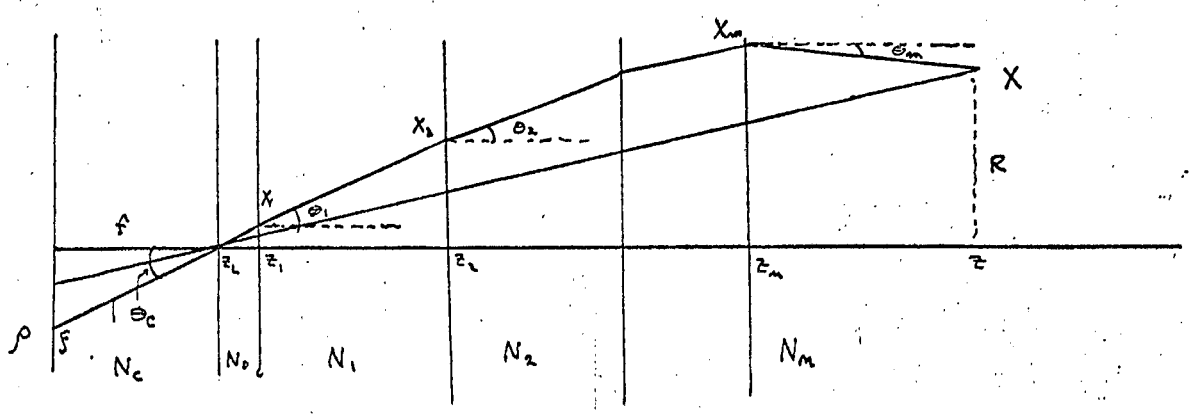

In the diagram, the optical path of a ray joining X and ξ is shown. The following points are identified:

x_i is the point at which the light ray passes through interface i.

R_i is the radial distance of x_i from the optic axis.

N_i is the index of refraction of material i.

f is the focal length of the lens.

ρ is the radial distance from ξ to the optic axis.

θ_i is the angle the ray makes with the normal at interface i.

Clearly

$$R_1 = \tan\theta_0 \, (Z_1 - Z_L)$$

$$R_2 - R_1 = \tan\theta_1 \, (Z_2 - Z_1)$$

$$\vdots \qquad\qquad \vdots$$

$$R - R_n = \tan\theta_n \, (Z - Z_n)$$

Thus

$$R = \sum_{i=0}^{n} \tan\theta_i (Z_{i+1} - Z_i) \overset{(1)}{=} \tan\theta_c \sum_{i=0}^{n} \frac{\tan\theta_i}{\tan\theta_c} (Z_{i+1} - Z_i)$$

where

$$Z_{n+1} = Z$$

But

$$\tan\theta_c = \rho/f$$

Hence

$$R = \frac{\rho}{f} \sum_{i=0} \frac{\tan\theta_i}{\tan\theta_c} (Z_{i+1} - Z_i)$$

From Snell's Law

$$N_c \sin\theta_c = N_0 \sin\theta_0 = \cdots = N_n \sin\theta_n$$

Hence

$$\frac{\tan\theta_i}{\tan\theta_c} = \frac{N_c/N_i}{\left[1+(1-(\frac{N_c}{N_i})^2)\tan^2\theta_c\right]^{1/2}} = \frac{N_c/N_i}{\left[1+(1-(\frac{N_c}{N_i})^2)\,(\frac{\rho}{f})^2\right]^{1/2}}$$

Define

$$r_i = (1 - (\frac{N_c}{N_i})^2)\,(\frac{\rho}{f})^2$$

$$g_i(\rho) = \frac{\tan\theta_i}{\tan\theta_c} = \frac{N_c}{N_i}\left[1 - \frac{1}{2} r_i + \frac{3}{8} r_i^2 - \cdots\right] \overset{(2)}{}$$

---

1. Note that all terms for a given refractive material can be grouped. Thus it is only necessary to have one term for each distinct refractive material.
2. For all chambers currently being processed, $g_i(\rho)$ can be truncated after r_i^2.

Define

$$G(\rho,Z) = \sum_{i=1}^{n} g_i(\rho)\left(\frac{Z_{i+1} - Z_i}{f}\right)$$

Then

$$R = \rho G(\rho,Z)$$

Now

$$X - X_L = R\cos\omega$$
$$Y - Y_L = R\sin\omega$$

Hence

$$X - X_L = \rho\cos\omega G(\rho,Z)$$
$$Y - Y_L = \rho\sin\omega G(\rho,Z)$$

But since the optical path lies in a plane containing X and ξ and the optic axis we can write

$$\xi = \rho\cos\omega$$
$$\eta = \rho\sin\omega$$

Hence

$$X - X_L = -\xi G(\rho, Z)$$
$$Y - Y_L = -\eta G(\rho, Z)$$

For each view L we define a 2 component vector function $F_L(X, \xi)$ as follows:

$$F_L(X, \xi) = \begin{bmatrix} F_{1L}(X,\xi) \\ F_{2L}(X,\xi) \end{bmatrix} = \begin{bmatrix} X - X_L + \xi G(\rho,Z) \\ Y - Y_L + \eta G(\rho,Z) \end{bmatrix}$$

By setting $F_L(X,\xi) = 0$ we have the desired relationship between space coordinates X and film coordinates ξ.

Appendix C

Application of Lagrangian Constraints

Let

$$\xi_M = (\xi_{M_1} \ \eta_{M_1} \ \xi_{M_2} \ \eta_{M_2} \ \ldots\ldots)^T$$

$$\xi = (\xi_1 \ \eta_1 \ \xi_2 \ \eta_2 \ \ldots\ldots)^T$$

From the error analysis, an a priori estimate for the variance on each point is known.

Let

$$E = \begin{bmatrix} \sigma_{11}^2 & \sigma_{12}^2 & 0 & 0 & \ldots\ldots\ldots \\ \sigma_{21}^2 & \sigma_{22}^2 & 0 & 0 & \ldots\ldots\ldots \\ 0 & 0 & \sigma_{33}^2 & \sigma_{34}^2 & \ldots\ldots\ldots \\ 0 & 0 & \sigma_{43}^2 & \sigma_{44}^2 & \ldots\ldots\ldots \\ \vdots & \vdots & \vdots & \vdots & \end{bmatrix}$$

be the variance–covariance matrix of ξ_M.

One wishes to find a value for ξ such that

$$(\xi - \xi_M)^T E^{-1} (\xi - \xi_M) = \text{minimum} \qquad (1)$$

subject to the constraint

$$F_L(\xi_i, \bar{X}(s_i)) = 0 \qquad \xi_i \in \xi \qquad (2)$$

Define

$$s = (s_1\ s_2\ \ldots)^T$$

$$a = (p_v\ \alpha_v\ \beta_v\ X_v\ Y_v\ Z_v)^T\ *$$

$$F(\xi,\ s,\ a) = (F_1(\xi_1,\ \bar{X}(s_1))\ F_2(\xi_1,\ \bar{X}(s_1))\ F_1(\xi_2,\ \bar{X}(s_2))\ \ldots\ldots\ )^T$$

Then F can be expanded in a Taylor's series

$$F(\xi,\ s,\ a) = F_0 + \left(\frac{\partial F}{\partial \xi}\right)_0 \Delta\xi + \left(\frac{\partial F}{\partial s}\right)_0 \Delta s + \left(\frac{\partial F}{\partial a}\right)_0 \Delta a$$

Let γ represent the Lagrangian multipliers of F and let A be any non-singular matrix of rank equal to the dimension of γ.

Define

$$H(\xi,\ s,\ a) = AF(\xi,\ s,\ a) = H_0 + \left(\frac{\partial H}{\partial \xi}\right)_0 \Delta\xi + \left(\frac{\partial H}{\partial s}\right)_0 \Delta s + \left(\frac{\partial H}{\partial a}\right)_0 \Delta a$$

Conditions (1) and (2) will be satisfied provided

$$M = (\Delta\xi + \xi_0 - \xi_M)^T E^{-1} (\Delta\xi + \xi_0 - \xi_M) + 2 \left[H_0 + \left(\frac{\partial H}{\partial \xi}\right)_0 \Delta\xi + \left(\frac{\partial H}{\partial s}\right)_0 \Delta s + \left(\frac{\partial H}{\partial a}\right)_0 \Delta a\right]^T \gamma = \min \qquad (3)$$

---

* It is not possible to determine all of the variables X_v, Y_v, Z_v simultaneously. One of them must be specified. We choose to specify the component of $(X_v\ Y_v\ Z_v)$ corresponding to the largest component of λ_v. We use the value of this component determined by 2-view FOG. This will cause the resulting point of zero arc length to be quite close to the true vertex point in most cases. The final value of the vertex point is determined in CLOUDY.

A necessary and sufficient condition for (3) is

$$\text{(a)}\ \frac{\partial M}{\partial \Delta \xi} = 2E^{-1}(\xi_o + \Delta\xi - \xi_M) + 2\left(\frac{\partial H}{\partial \xi}\right)_o^T \gamma = 0$$

$$\text{(b)}\ \frac{\partial M}{\partial \Delta s} = \left(\frac{\partial H}{\partial s}\right)_o^T \gamma = 0 \qquad (4)$$

$$\text{(c)}\ \frac{\partial M}{\partial \Delta a} = \left(\frac{\partial H}{\partial a}\right)^T \gamma = 0$$

$$\text{(d)}\ \frac{\partial M}{\partial \gamma} = \left[H_o + \left(\frac{\partial H}{\partial \xi}\right)_o \Delta\xi + \left(\frac{\partial H}{\partial s}\right)_o \Delta s + \left(\frac{\partial H}{\partial a}\right)_o \Delta a = 0\right.$$

From (4a)

$$\Delta\xi = \xi_M - \xi_o - E\left(\frac{\partial H}{\partial \xi}\right)_o \gamma \qquad (5)$$

Substituting this result in (4d) gives

$$\left(\frac{\partial H}{\partial \xi}\right)_o E \left(\frac{\partial H}{\partial \xi}\right)_o^T \gamma = \left[H_o + \left(\frac{\partial H}{\partial s}\right)_o \Delta s + \left(\frac{\partial H}{\partial a}\right)_o \Delta a + \left(\frac{\partial H}{\partial \xi}\right)_o (\xi_M - \xi_o)\right]$$

We choose A such that

$$\left(\frac{\partial H}{\partial \xi}\right)_o E \left(\frac{\partial H}{\partial \xi}\right)_o^T = A \left(\frac{\partial F}{\partial \xi}\right)_o E \left(\frac{\partial F}{\partial \xi}\right)_o^T A^T = I$$

Hence

$$\gamma = H_o + \left(\frac{\partial H}{\partial s}\right)_o \Delta s + \left(\frac{\partial H}{\partial a}\right)_o \Delta a + \left(\frac{\partial H}{\partial \xi}\right)_o (\xi_M - \xi_o) \qquad (6)$$

Substituting this result in (4b) and (4c) gives

$$\left(\frac{\partial H}{\partial s}\right)_o^T \left(\frac{\partial H}{\partial s}\right)_o \Delta s + \left(\frac{\partial H}{\partial s}\right)_o^T \left(\frac{\partial H}{\partial a}\right)_o \Delta a = -\left(\frac{\partial H}{\partial s}\right)_o^T \left(H_o + \left(\frac{\partial H}{\partial \xi}\right)_o (\xi_M - \xi_o)\right)$$

$$\left(\frac{\partial H}{\partial a}\right)_o^T \left(\frac{\partial H}{\partial s}\right)_o \Delta s + \left(\frac{\partial H}{\partial a}\right)_o^T \left(\frac{\partial H}{\partial a}\right) \Delta a = -\left(\frac{\partial H}{\partial a}\right)_o^T \left(H_o + \left(\frac{\partial H}{\partial \xi}\right)_o (\xi_M - \xi_o)\right)$$

from which the following equations can be deduced:

Define

$$B = \left(\frac{\partial H}{\partial a}\right)_o^T \left(I - \left(\frac{\partial H}{\partial s}\right)_o \left[\left(\frac{\partial H}{\partial s}\right)_o^T \left(\frac{\partial H}{\partial s}\right)_o\right]^{-1} \left(\frac{\partial H}{\partial s}\right)_o^T\right)$$

Then

$$\Delta a = - \left[B \left(\frac{\partial H}{\partial a} \right)_o \right]^{-1} B \left[Ho + \left(\frac{\partial H}{\partial \xi} \right)_o (\xi_M - \xi_o) \right] \tag{7}$$

$$\Delta s = - \left[\left(\frac{\partial H}{\partial s} \right)^T_o \left(\frac{\partial H}{\partial s} \right)_o \right]^{-1} \left[\left(\frac{\partial H}{\partial s} \right)^T_o \left(Ho + \left(\frac{\partial H}{\partial \xi} \right)_o (\xi_M - \xi_o) \right) + \left(\frac{\partial H}{\partial s} \right)^T_o \left(\frac{\partial H}{\partial a} \right)_o \Delta a \right] \tag{8}$$

Thus starting from a first guess ξ_o, s_o, a_o improvements $\Delta\xi$, ΔS, Δa can be computed as follows:

(a) Compute $F_o, \left(\frac{\partial F}{\partial \xi} \right)_o, \left(\frac{\partial F}{\partial s} \right)_o, \left(\frac{\partial F}{\partial a} \right)_o$ (9)

(b) Compute A so that

$$A \left(\frac{\partial F}{\partial \xi} \right)_o E \left(\frac{\partial F}{\partial \xi} \right)^T_o A^T = I \quad \text{(See (10) below.)}$$

(c) Compute $H_o = AF_o$

$$\left(\frac{\partial H}{\partial \xi} \right)_o = A \left(\frac{\partial F}{\partial \xi} \right)_o$$

$$\left(\frac{\partial H}{\partial s} \right)_o = A \left(\frac{\partial F}{\partial s} \right)_o$$

$$\left(\frac{\partial H}{\partial a} \right)_o = A \left(\frac{\partial F}{\partial a} \right)_o$$

(d) Compute Δa from (7)

(e) Compute Δs from (8)

(f) Compute γ from (6)

(g) Compute $\Delta\xi$ from (5)

There are an infinite number of matrices A which satisfy (b). Since

$$\left(\frac{\partial F}{\partial \xi} \right)_o E \left(\frac{\partial F}{\partial \xi} \right)^T_o$$

has the following block diagonal form,

$$\left(\frac{\partial F}{\partial \xi} \right)_o E \left(\frac{\partial F}{\partial \xi} \right)^T = \begin{bmatrix} a_{11} & a_{12} & 0 & 0 & \cdots \\ a_{12} & a_{22} & 0 & 0 & \cdots \\ 0 & 0 & a_{33} & a_{34} & \cdots \\ 0 & 0 & a_{34} & a_{44} & \cdots \\ \vdots & \vdots & \vdots & \vdots & \end{bmatrix}$$

A particularly simple solution is

$$A = \begin{bmatrix} \underbrace{\begin{matrix} \frac{1}{\sqrt{a_{11}}} & 0 \\ \frac{-a_{12}}{a_{11}\sqrt{a_{11}}} & \frac{1}{(a_{22}-a_{21}^2/a_{14})^{1/2}} \\ 0 & 0 \\ 0 & 0 \\ \vdots & \vdots \end{matrix}}_{\text{if } a_{11} \geq a_{22}} & \underbrace{\begin{matrix} 0 & 0 \ldots \\ 0 & 0 \ldots \\ \frac{1}{(a_{33}-a_{34}^2/a_{44})^{1/2}} & \frac{-a_{34}}{a_{44}\sqrt{a_{44}}} \\ 0 & \frac{1}{\sqrt{a_{44}}} \ldots \\ \vdots & \vdots \ldots \end{matrix}}_{\text{if } a_{44} \geq a_{33}} \end{bmatrix} \quad (10)$$

Clearly some of the matrices in the above procedure are quite large. For example, for a track with 20 points in each view $\left(\frac{\partial F}{\partial \xi}\right)_o E\left(\frac{\partial F}{\partial \xi}\right)^T$ would contain 120 x 120 or 14,400 elements. Fortunately, nearly all of the elements are zero. In fact, for this example, only 240 of the elements are non zero.

In general, all of the large matrices are in block diagonal form where the individual blocks are made up of (1 x 1), (1 x 2), or (2 x 2) matrices. This simply means that special block diagonal matrix routines must be used in carrying out the iterative procedure.

Appendix D

Derivation of a Simple Error Expression for Vertex Points

For each track j at a vertex there is an orbit function $\bar{X}^j(s)$. The point X in space which is the closest to all of these functions is taken to be the vertex point.

Specifically, the points s_j are found such that

$$\sum_j \left| X - \bar{X}(s_j) \right|^2 = \text{minimum} \tag{1}$$

Let

$$\begin{aligned} X_j &= \bar{X}^j(s_j) \\ \lambda_j &= \bar{\lambda}^j(s_j) \end{aligned} \tag{2}$$

(See Appendix A for definitions of $\bar{X}$ and $\bar{\lambda}$.)

The distance δ_j of a point X from the line passing through X_j with direction cosines λ_j is given by

$$\delta_j = \lambda_j^T (X - X_j) \tag{3}$$

The requirement of

$$\sum_j \delta_j^2 = \text{minimum}$$

implies

$$X = \left[\sum_j \left[\lambda_j \lambda_j^T \right] \right]^{-1} \sum_j \lambda_j \lambda_j^T X_j \tag{4}$$

Hence

$$\frac{\partial X}{\partial X_j} = \left[\sum_j \lambda_j \lambda_j^T \right]^{-1} \lambda_j \lambda_j^T \tag{5}$$

Assume

$$E_{\lambda_j} = {}^2 I \text{ and } E_{\lambda_j} = 0$$

Then

$$E_X = \sum_j \left(\frac{\partial X}{\partial X_j}\right) (I\ {}^2) \left(\frac{\partial X}{\partial X_j}\right)^T = {}^2 \left[\sum_j \lambda_j \lambda_j^T \right]^{-1} \tag{6}$$

As an example, consider the simple case of two tracks in the x y plane.

Let $$\lambda_1 = (\cos \Theta_1, \sin \Theta_1)^T$$

$$\lambda_2 = (\cos \Theta_2, \sin \Theta_2)^T$$

$$E_{X_j} = \begin{pmatrix} 2 & 0 \\ 0 & 2 \end{pmatrix}$$

Then from (6)

$$E_X = 2\left[\sum_j \lambda_j \lambda_j^T \right]^{-1}$$

Therefore

$$E_X = \frac{2}{\sin^2 (\Theta_2 - \Theta_1)} \begin{pmatrix} \cos^2 \Theta_1 + \cos^2 \Theta_2 & -(\cos \Theta_1 \sin \Theta_1 + \cos \Theta_2 \sin \Theta_2) \\ -(\cos \Theta_1 \sin \Theta_1 + \cos \Theta_2 \sin \Theta_2) & \sin^2 \Theta_1 + \sin^2 \Theta_2 \end{pmatrix}$$

Clearly

$$E_X \to \infty \text{ as } |\Theta_2 - \Theta_1| \to 0$$

and

$$E_X \to 2 I \text{ as } |\Theta_2 - \Theta_1| \to \pi/2$$

Thus, in this case, E_X behaves as would be expected.

References

1. Solmitz, Day and Johnson. Three View Geometry Program, Alvarez Group Programmers Note, University of California, Lawrence Radiation Laboratory, Berkeley, p. 117.

2. Rossi. High Energy Particles. Prentice-Hall, 1956

3. Mood. Introduction to the Theory of Statistics. McGraw-Hill, 1950.

4. Hough. "On Getting Results from an HPD System." Paper delivered at Purdue Conference on Instrumentation for High Energy Physics, May 1965.